Magnetic susceptibility and heat capacity measurements of single crystal $TbMnO_3$

2014 J. Phys.: Condens. Matter 26 256002

(http://iopscience.iop.org/0953-8984/26/25/256002)

IOP Publishing Journal of Physics: Condensed Matter
J. Phys.: Condens. Matter **26** (2014) 256002 (6pp) doi:10.1088/0953-8984/26/25/256002

Magnetic susceptibility and heat capacity measurements of single crystal $TbMnO_3$

D O'Flynn[1], M R Lees and G Balakrishnan

Department of Physics, University of Warwick, Coventry CV4 7AL, UK

E-mail: d.oflynn@ucl.ac.uk, m.r.lees@warwick.ac.uk and g.balakrishnan@warwick.ac.uk

Received 15 January 2014, revised 17 March 2014
Accepted for publication 1 April 2014
Published 27 May 2014

Abstract

Measurements of the magnetic susceptibility χ and heat capacity C on single crystals of the multiferroic $TbMnO_3$ are presented. A non-magnetic isostructural compound, $LaGaO_3$, was used to isolate the magnetic component of the heat capacity. An anisotropic magnetic susceptibility, deviations from Curie-Weiss behaviour and a significant magnetic entropy above the antiferromagnetic ordering temperature $T_{N1} = 41$ K are attributed to a combination of crystal-field effects and short-range order between the Mn moments. Heat capacity in a magnetic field applied along the a axis confirms the saturation of Tb^{3+} moments in 90 kOe. A hyperfine contribution from the Tb and Mn nuclear moments that may be convolved with a contribution from low-lying Tb crystal-field levels leads to a low-temperature rise in $C(T)/T$.

Keywords: multiferroics, antiferromagnetism, magnetic susceptibility, heat capacity, single crystal

(Some figures may appear in colour only in the online journal)

1. Introduction

In recent years, multiferroic materials have attracted significant interest due to the coexistence of (anti)ferromagnetism and ferroelectricity [1–3]. The discovery of strong coupling between these properties makes multiferroics potentially attractive for technological applications [4–7]. A well studied multiferroic compound is $TbMnO_3$, which shows coincident antiferromagnetic and ferroelectric order [8–13]. Importantly, it is possible to change the electric polarization direction in this compound by the application of a magnetic field [2].

$TbMnO_3$ (space group *Pbnm*) undergoes three distinct magnetic transitions. At $T_{N1} = 41$ K, the Mn^{3+} moments show sinusoidal antiferromagnetic order propagating along the crystallographic b axis [2]. The Mn^{3+} moments undergo a further transition at $T_{N2} = 27$ K, with the moments arranging in a cycloid in the b-c plane. It is this magnetic order which breaks inversion symmetry and results in a ferroelectric polarization developing at the same temperature [8, 9, 14, 15]. At $T_{N3} = 7$ K, the Tb^{3+} moments order antiferromagnetically [16, 17]. An x-ray resonant scattering study gave a refinement of the magnetic structure of the Mn^{3+} moments, with a canting in the c direction in the sinusoidal order phase and a canting in the a direction in the cycloidal order phase [18].

There is a strong coupling between the Mn and Tb moments. The magnetization versus applied magnetic field data at low temperature for single crystal $TbMnO_3$ show two sharp metamagnetic transitions with the field applied along the b axis and are described as being due to reversal of the Tb moments [2]. The second transition at ~50 kOe coincides with the ferroelectric polarization flop from the c to the a axis [19]. There is a change in the orientation of the Mn moments from a b-c to an a-b cycloidal ordering under these magnetic field conditions, highlighting the strong coupling between the Mn and the Tb moments and explaining the resultant modifications to the ferroelectric properties of $TbMnO_3$ [20].

$TbMnO_3$ has been studied in some detail. Despite this, there are still only limited data available for some important bulk properties. The temperature dependence of the magnetic susceptibility χ has been reported over a restricted temperature range along some crystallographic directions for single crystals [2, 19, 21, 22] and thin films [23] while heat capacity C as a function of temperature has been reported in zero magnetic field for crystals [2, 22] and in magnetic field for polycrystalline $TbMnO_3$ [24]. This work aims to fill these gaps in

[1] Author to whom any correspondence should be addressed. Department of Medical Physics and Bioengineering, University College London, WC1E 6BT, UK

the literature. Detailed measurements of the magnetic susceptibility of single crystals of $TbMnO_3$ are presented along the three principal crystallographic axes and an analysis using the Curie–Weiss law is given. We also present heat capacity data with magnetic fields from 0–90 kOe applied along the *a* axis, as well as low-temperature measurements down to 0.6 K. The non-magnetic isostructural compound, $LaGaO_3$, was used to try to isolate the magnetic contribution to the heat capacity of $TbMnO_3$. The magnetic susceptibility and heat capacity measurements reveal that short-range magnetic order persists above T_{N1} and that significant crystal-field (CF) effects are present in this material up to 200 K.

2. Experimental details

A single crystal of $TbMnO_3$ was grown at a rate of 10 mm h^{-1} using the floating zone method. The growth was carried out in an Ar atmosphere, using protocols based on previous work [19]. For magnetic dc susceptibility measurements a single crystal piece was cut into a rectangular cuboid with dimensions ~2 × 2 × 3 mm^3, with each surface normal parallel to a principal crystallographic axis. For the heat capacity measurements, a single crystal was cut into a thin plate of ~2 × 2 × 0.5 mm^3, with the normal to the plate parallel to the *a* axis. Polycrystalline $LaGaO_3$ was prepared by reacting stoichiometric ratios of La_2O_3 and Ga_2O_3. The resulting powder was then pressed into a pellet before sintering at 1400 °C. Magnetic susceptibility measurements were made using a Quantum Design Magnetic Property Measurement System (MPMS) XL SQUID magnetometer and the heat capacity was measured with a Quantum Design Physical Property Measurement System (PPMS).

3. Results

3.1. Magnetic susceptibility

The magnetic susceptibility, χ, of $TbMnO_3$ is highly anisotropic indicating the presence of significant crystal-field effects. Figure 1 shows the zero-field-cooled warming (ZFCW) and field-cooled cooling (FCC) χ (*T*) data with a field *H* = 1 kOe applied along each of the three principal crystallographic axes. At low temperatures the largest susceptibility is seen for a magnetic field applied parallel to the *a* axis, the direction along which the Tb^{3+} moments have been shown to order in low magnetic field [19], and suggests that at lower temperatures the Tb^{3+} are constrained to lie preferentially along this axis. The susceptibility along the *c* axis exhibits peaks at temperatures corresponding to the magnetic transitions in $TbMnO_3$ at T_{N1} and T_{N1}. This is the only direction along which there is a clear signature in $\chi(T)$ for the ordering of the Mn moments. Features are seen in the susceptibility along each of the three principal crystallographic direction around T_{N3} = 7 K, corresponding to the independent magnetic order of the Tb^{3+} moments. For $H\|a$ and *b* the susceptibility is almost reversible while for $H\|c$ there is a clear hysteresis between the ZFCW and FCC data around T_{N3}. The observed magnetic susceptibility shows similar behaviour to those published for $Tb_{0.8}Y_{0.2}MnO_3$ [25] and $Tb_{0.95}Bi_{0.05}MnO_3$ [26], and for $TbMnO_3$ up to 60 K

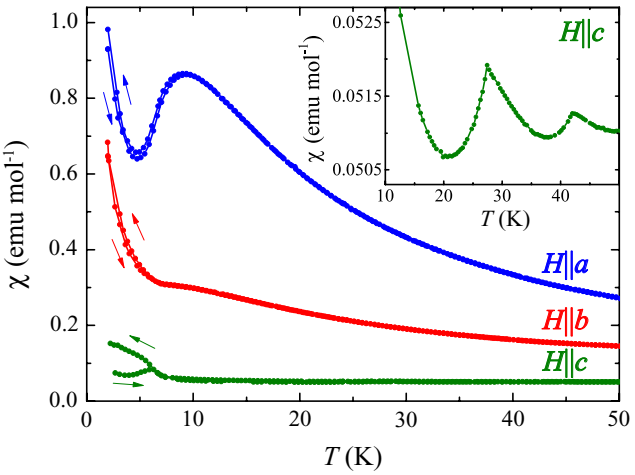

Figure 1. Magnetic dc susceptibility measured as a function of temperature in a magnetic field of 1 kOe applied along the principal crystallographic axes of a $TbMnO_3$ single crystal. Arrows indicate the ZFCW and FCC data. Inset: expanded view of the ZFCW susceptibility for $H\|c$.

[11, 21]. Choosing the maximum in χ (*T*) at 9 K with $H\|a$ and *b* accounts for the higher value for T_{N3} reported in [21].

In order to conduct a quantitative analysis of the magnetic susceptibility data, measurements in an applied field of 5 kOe were taken between 2 K and 400 K (figure 2). The inverse susceptibility in the paramagnetic regime was then fitted to the Curie–Weiss (CW) law. A CW dependence is not seen along any of the three directions measured until temperatures much higher than T_{N1} = 41 K. Particularly interesting susceptibility data was measured with $H\|c$, where CW behaviour was not observed until temperatures around 200 K above T_{N1}. Instead, a broad maximum is present between ~40 and 250 K. The results of these fits are shown in table 1. Since the magnetic susceptibility is made up of contributions from both the Tb^{3+} and Mn^{3+} moments, it is difficult to separate the contributions of each ion from this data. As such, the values of the effective magnetic moment $p_{eff} = \mu/\mu_B$ determined, represent the overall moment per formula unit μ of $TbMnO_3$ and is given by $p_{eff}^2(TbMnO_3) = p_{eff}^2(Tb) + p_{eff}^2(Mn)$. For comparison with the values given in table 1, the theoretical effective moment of $TbMnO_3$ was calculated as $p_{eff}^2 = \left[g_{J_{Tb}}^2 (J_{Tb}(J_{Tb}+1)) + g_{J_{Mn}}^2 (J_{Mn}(J_{Mn}+1)) \right] = 10.89$ where $g_{J_{Tb}}$ and $g_{J_{Mn}}$ are the Landé *g* values and J_{Tb} and J_{Mn} are the total angular momentum for the Tb^{3+} and Mn^{3+} ions respectively. (It should be noted that the errors given for the values of *C*, θ and p_{eff} are the statistical errors from the fits to the data). There is reasonable agreement between the values of p_{eff} found along the *a*, *b* and *c* axes and the expected value. As a result of the magnetic anisotropy the values of θ are also quite different along the three principal crystallographic axes, with no value being close to $-T_{N1} = -41$ K.

A Curie-Weiss analysis has previously been carried out on polycrystalline $TbMnO_3$ [27]. In order to compare our results with this published data and to validate the single crystal data presented above, a piece of single crystal $TbMnO_3$ was crushed into polycrystalline form for susceptibility measurement. The polycrystalline susceptibility is shown in figure 3, alongside a crystal average calculated as $(\chi_a + \chi_b + \chi_c)/3$ (where χ_a, χ_b and χ_c are the susceptibilities along the *a*, *b* and

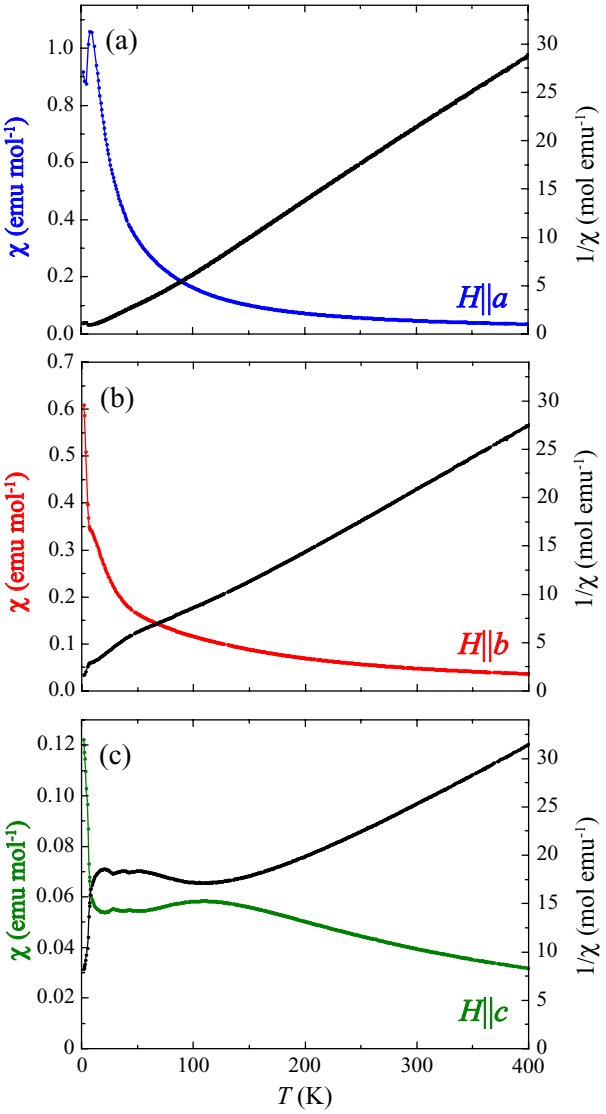

Figure 2. Magnetic dc susceptibility and inverse susceptibility as a function of temperature for $TbMnO_3$, along the (*a*) *a* axis, (*b*) *b* axis and (*c*) *c* axis. Measurements were made in an applied magnetic field of 5 kOe.

c axis respectively). An effective moment of 10.72(1) was measured for the polycrystalline sample, in good agreement with the theoretical value and the value of 10.95 reported previously [27]. The inverse susceptibility data is linear from 60 K upwards, a temperature which is much closer to T_{N1} than for the single crystal data. The value for θ was calculated as −21.9 K for the polycrystalline sample. The crystal average of the susceptibility data gives similar results to the polycrystalline data. The CW analysis of this data gave p_{eff} = 10.87(1), which is very close to the theoretical value of 10.89 calculated above. Fitting the crystal average data over the temperature range 60–400 K does not significantly affect the results of the analysis, with θ = −31.7(1) K and p_{eff} = 10.88(1) in this case.

The magnetic susceptibility data indicate that immediately above T_{N1}, a combination of crystal-field effects and perhaps short-range order between the Mn moments modify the magnetic response and that a CW behaviour is only seen at temperature in excess of 200 K. Inelastic neutron scattering

Table 1. Curie constant, *C*, Weiss temperature, θ and effective magnetic moment, p_{eff}, for $TbMnO_3$(T_{N1} = 41 K) obtained from Curie-Weiss fits to the inverse susceptibility versus temperature for a single crystal, a crystal average calculated as $(\chi_a + \chi_b + \chi_c)/3$ and powder from a crushed crystal piece. The expected p_{eff} value for $TbMnO_3$ is 10.89. The significant differences in θ for $H\|a$, *b* and *c* are due to effects of the crystal fields.

	C (emu K mol^{-1})	θ (K)	p_{eff}	Fit range (K)
$H\|\|a$	13.33(1)	+17.6(2)	10.32(1)	100–400
$H\|\|b$	15.15(2)	−9.3(5)	11.00(1)	200–400
$H\|\|c$	16.75(5)	−128(1)	11.57(2)	250–400
Crystal average	14.78(1)	−30.8(1)	10.87(1)	250–400
Polycrystalline	14.38(1)	−21.9(1)	10.72(1)	60–400

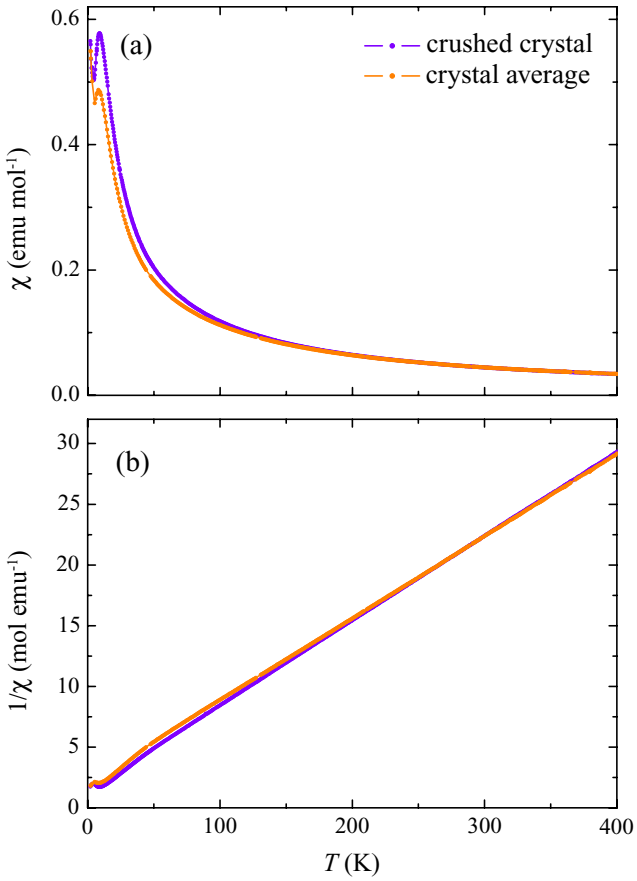

Figure 3. (*a*) Magnetic dc susceptibility and (*b*) inverse susceptibility versus temperature for polycrystalline $TbMnO_3$ and an average of the data along the *a*, *b* and *c* axes. Measurements were made in an applied magnetic field of 5 kOe.

has suggested that $TbMnO_3$ has a crystal-field excitation at around 4.50 meV (52.2 K) but there is no detailed crystal-field scheme published for this material [28, 29]. In the absence of such information it is not practical to calculate how the CF effects will modify the magnetic susceptibility of $TbMnO_3$.

3.2. Heat capacity

The temperature dependence of the heat capacity for $TbMnO_3$ in different applied magnetic fields is shown in figure 4. For practical reasons, the magnetic field was

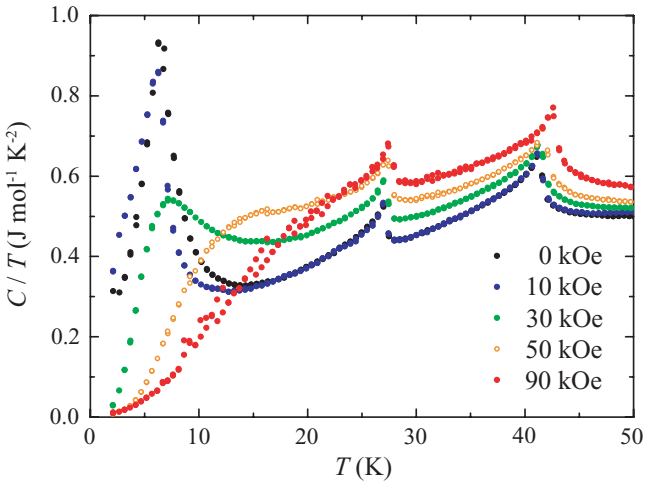

Figure 4. Specific heat capacity divided by temperature versus temperature for a single crystal of $TbMnO_3$, with magnetic fields applied along the *a* axis.

applied along the *a* axis. This is the magnetic 'easy' axis for $TbMnO_3$ [16, 19], and therefore reduced the risk of damage to the delicate PPMS heat capacity sample stage from any magnetic torque on the crystal. As previously reported, there are three distinct peaks in the zero-field specific heat, corresponding to the magnetic transitions at T_{N1}, T_{N2} and T_{N3} [2]. For successively higher applied magnetic fields, there is a gradual smearing out of the low-temperature peak corresponding to the ordering of the Tb^{3+} moments until it has nearly completely disappeared at 90 kOe (the highest field the PPMS is capable of achieving). This implies that a magnetic field of 90 kOe is sufficient to force the Tb^{3+} moments into the saturated paramagnetic state. A measurement of the heat capacity versus applied magnetic field at 3 K (figure 5(*a*)) shows a peak at ~20 kOe. This behaviour is reflected by the metamagnetic transition seen in $TbMnO_3$ with a similar magnetic field applied along the *a* axis [19]. Another change in the heat capacity due to an applied magnetic field is the shift of the Mn^{3+} ordering peak at T_{N1} towards higher temperature. This behaviour was also reported in the phase diagram of $TbMnO_3$, from measurements of the dielectric constant [19]. The heat capacity is still weakly field dependent at 60 K, i.e. in the paramagnetic state (figure 5(*b*)).

In order to determine the magnetic contribution to the heat capacity of $TbMnO_3$, the heat capacity of the non-magnetic isostructural material $LaGaO_3$ was measured as a function of temperature to estimate the lattice contribution to the heat capacity. The results of these measurements are shown in figure 6. Since the $LaGaO_3$ and $TbMnO_3$ compounds have different molecular masses, the temperatures for the $LaGaO_3$ data were normalized by multiplying by the ratio of the effective Debye temperatures of the two compounds, using the method adopted by Bouvier *et al* [30]. with

$$\frac{\Theta_D(\mathrm{TbMnO_3})}{\Theta_D(\mathrm{LaGaO_3})} = \left[\frac{(M_{\mathrm{La}})^{\frac{3}{2}} + (M_{\mathrm{Ga}})^{\frac{3}{2}} + 3(M_{\mathrm{O}})^{\frac{3}{2}}}{(M_{\mathrm{Tb}})^{\frac{3}{2}} + (M_{\mathrm{Mn}})^{\frac{3}{2}} + 3(M_{\mathrm{O}})^{\frac{3}{2}}}\right]^{\frac{1}{3}}, \quad (1)$$

where Θ_D is the Debye temperature and M is the atomic mass of each of the constituent atoms. A correction factor of

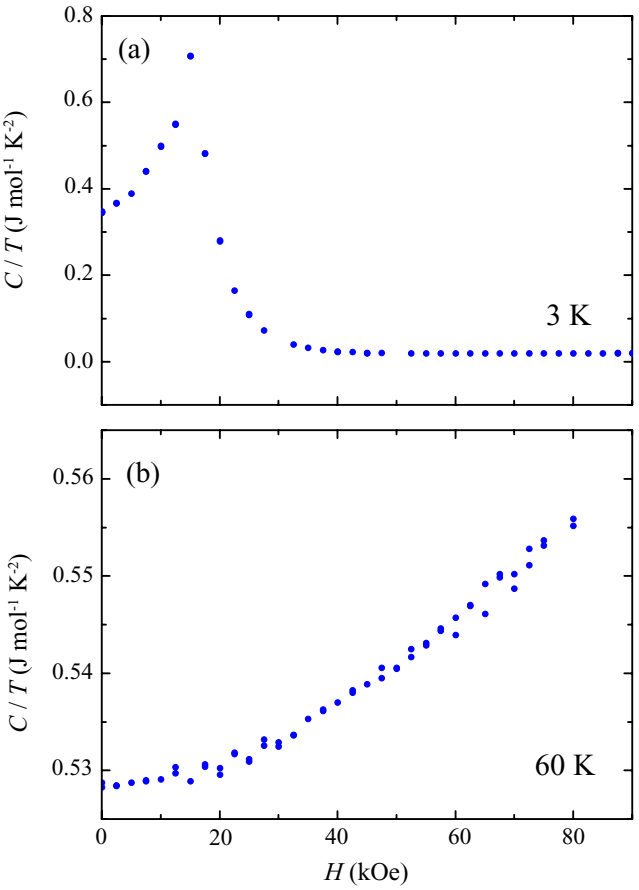

Figure 5. Specific heat divided by temperature versus magnetic field along the *a* axis for a single crystal of $TbMnO_3$, at (*a*) 3 K and (*b*) 60 K.

0.975 was applied to the $LaGaO_3$ temperature values. It can be seen that there is a non-zero value for the magnetic specific heat—and therefore magnetic entropy—up to 200 K, over 160 K higher than the magnetic ordering temperature T_{N1} = 41 K. This suggests that short-ranged magnetic correlations persist in $TbMnO_3$ at temperatures well above T_{N1}. The magnetic contribution to the heat capacity, $C_{\mathrm{mag}}(T)/T$ was integrated with respect to temperature to determine the magnetic entropy, S_{mag}. For this calculation a point was added to the data before integration at zero temperature and zero heat capacity. The measured magnetic entropy reached a saturation at ~23.4 J mol^{-1} K^{-1}, well below the theoretical maximum entropy of 34.7 J mol^{-1} K^{-1} calculated for $TbMnO_3$ using

$$S_{\mathrm{mag}}(\mathrm{TbMnO_3}) = R\ln(2J_{\mathrm{Tb^{3+}}}+1) + R\ln(2S_{\mathrm{Mn^{3+}}}+1). \quad (2)$$

To confirm that this discrepancy was not due to a large amount of magnetic entropy below 2 K, the heat capacity was measured down to 0.6 K using a He-3 PPMS sample insert (figure 7). A rapid increase in $C(T)/T$ is seen below 2 K, which appears to be the tail of a peak located below the temperature range of the measurement. The entropy associated with this low-temperature feature amounts to at least 0.7 J mol^{-1} K^{-1} in zero field. Again, a point was added to the data at zero temperature and zero heat capacity before integration. When this contribution is considered, the entropy in zero field saturates at ~24.1 J mol^{-1} K^{-1}(figure 8). A similar temperature

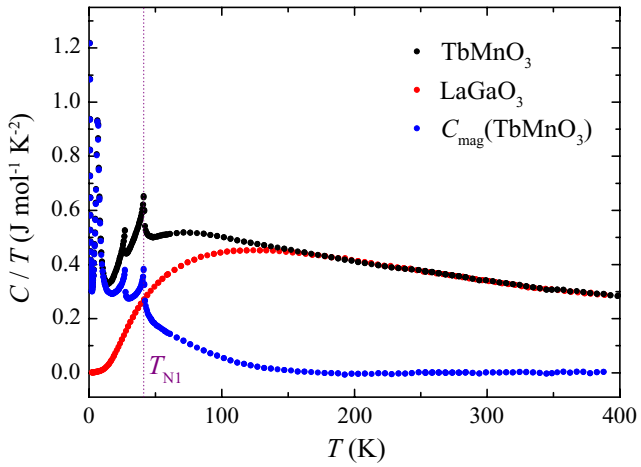

Figure 6. Specific heat divided by temperature versus temperature in zero applied magnetic field for a single crystal of $TbMnO_3$, a polycrystalline sample of the non-magnetic isostructural $LaGaO_3$ and the magnetic specific heat, calculated as $C_{mag}(TbMnO_3) = C(TbMnO_3) - C(LaGaO_3)$.

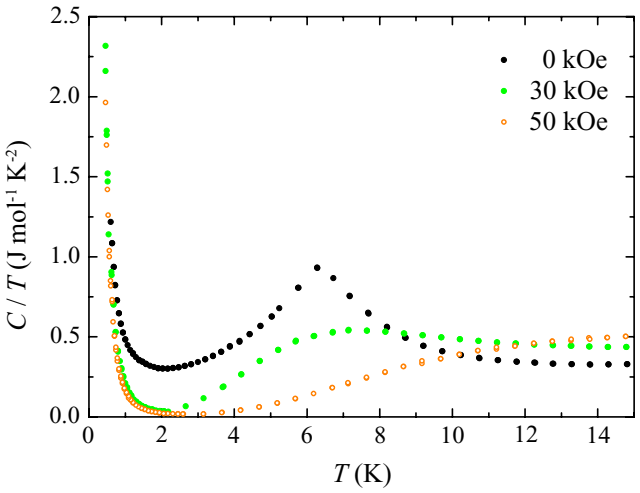

Figure 7. Low-temperature C/T versus T for a single crystal of $TbMnO_3$, with magnetic fields applied along the a axis.

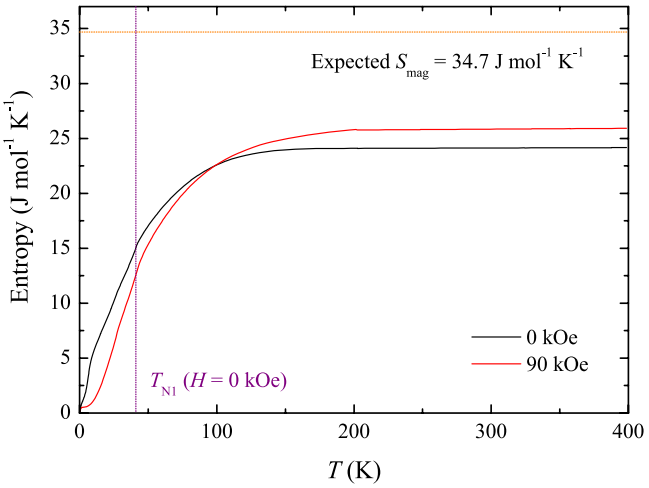

Figure 8. Magnetic entropy versus temperature for $TbMnO_3$ in magnetic fields of 0 and 90 kOe applied along the a axis. The horizontal dotted line shows the expected maximum entropy, calculated from equation (2).

dependence for $S_{mag}(T)$ is seen in a field of 90 kOe with $S_{mag}(T)$ still saturating well below the theoretical maximum entropy.

This low-temperature peak in $C/T(T)$ may be the result of a reorientation of the Tb moments at $T < T_{N3}$ as reported in $TbFeO_3$ and $TbCrO_3$ [31]. Low-temperature studies using a probe such as neutron scattering are required to verify this possibility. The weak magnetic field dependence of this feature suggests it may be a Schottky peak. Such a peak can arise from a hyperfine contribution to the heat capacity and is expected to scale as A/T^2 at temperatures above the Schottky anomaly, with the coefficient A being related to the hyperfine field, H_{hf} by

$$A = \frac{\mu_I^2 \mu_N^2 R}{3k_B^2}\left(\frac{I+1}{I}\right)H_{hf}^2, \qquad (3)$$

where I and μ_I are the nuclear spin quantum number and the nuclear magnetic moment of the ion respectively, R is the molar gas constant (8.314 J mol^{-1} K^{-1}) and μ_N is the nuclear magneton [32, 33]. Fitting to the zero-field low-temperature heat capacity data gave a value for A of 0.2027(7) J K mol^{-1}. For Tb, I = 3/2 and μ_I = 1.5 [33]. Putting these values into equation (3) gives H_{hf} = 3820 kOe. If instead the hyperfine contribution is assumed to be due to the Mn ions (with I = 5/2 and μ_I = 3.461), the hyperfine field is calculated as 1810 kOe. These fields are about an order of magnitude larger than the values quoted in the literature for Mn ions in either $La_{1-x}Sr_xMnO_3$ or Sr doped $Pr_{0.6}Ca_{0.4}MnO_3$ manganite [34, 35]. The large hyperfine fields are more likely to be due to electrons in the well screened unfilled 4f shell of the Tb ions being in reasonable agreement with the values of 3120(20) and 3205(5) kOe previously reported for Tb in $Tb_2Fe_{17}C_x$ and $TbAl_2$ respectively [36, 37].

Alternatively, this Schottky anomaly may result from the CF levels of the Tb ions. For example, in $Tb(OH)_3$ the low-temperature heat capacity contains a feature that is attributed to low lying crystal-field levels and hyperfine field contributions [38].

We also note that in some other Tb based materials, for example $TbFe_2$, the magnetic exchange field significantly modifies the CF energy level diagram leading to a large reduction in the contribution to the magnetic entropy at lower temperatures [39]. For $TbFe_2$, only $0.62R\ln(2J_{Tb^{3+}}+1)$ is seen by 300 K. The ordering temperature in $TbMnO_3$ is significantly lower but similar effects may still modify the CF scheme. Assuming there is a full contribution to the magnetic entropy from the Mn moments, we only observe $0.47R\ln(2J_{Tb^{3+}}+1)$ up to 300 K. However, a detailed knowledge of the CF levels in $TbMnO_3$ is required in order to build a more quantitative model of the contributions to $C_{mag}(T)$ from hyperfine and CF effects.

It is proposed that the main reasons why the measured magnetic entropy appears lower than expected are CF effects which modify the magnetic contribution to the heat capacity of the Tb moments, short-range correlations between the Mn moments persisting well into the paramagnetic state above T_{N1} and perhaps an overestimate in the lattice contribution to the

specific heat. This suggestion is consistent with the deviations from CW behaviour seen in the magnetic susceptibility data.

4. Conclusions

The magnetic behaviour of $TbMnO_3$ is highly anisotropic. The magnitude of the magnetic susceptibility in the paramagnetic state suggests that the Tb^{3+} moments are constrained to lie preferentially along the *a* axis. The deviations from CW behaviour observed below 200 K and the heat capacity show that CF effects and short-range correlations modify the magnetic response above T_{N1}. Although $TbMnO_3$ is one of the most widely studied multiferroic compounds, there is little discussion about the role of crystal-field effects in the magnetoelectric coupling exhibited by this material. Clear evidence for magnetic ordering of the Mn moments below T_{N1} is only seen for $H\|c$. This is the same crystallographic direction along which the spontaneous electric polarization develops below T_{N1}. Heat capacity measurements in an applied magnetic field confirm the proposal that the magnetization saturation seen for $H\|a$ is due to the Tb moments [19].

Acknowledgments

This work was supported by the Engineering and Physical Sciences Research Council (EPSRC), UK (EP/I007210/1). Some of the equipment used in this research was obtained through the Science City Advanced Materials project: Creating and Characterizing Next Generation Advanced Materials project, with support from Advantage West Midlands (AWM) and part funded by the European Regional Development Fund (ERDF). We wish to thank T E Orton for technical support.

References

[1] Wang J *et al* 2003 *Science* **299** 1719
[2] Kimura T, Goto T, Shintani H, Ishizaka K, Arima T and Tokura Y 2003 *Nature* **426** 55
[3] Hur N, Park S, Sharma P A, Ahn J S, Guha S and Cheong S W 2004 *Nature* **429** 392
[4] Ramesh R and Spaldin N A 2007 *Nature Mater.* **6** 21
[5] Zavaliche F *et al* 2005 *Nano Lett.* **5** 1793
[6] Vopsaroiu M, Blackburn J and Cain M G 2007 *J. Phys. D: Appl. Phys.* **40** 5027
[7] Zhang Y, Li Z, Deng C, Ma J, Lin Y and Nan C W 2008 *Appl. Phys. Lett.* **92** 152510
[8] Xiang H J, Wei S H, Whangbo M H and Da Silva J L F 2008 *Phys. Rev. Lett.* **101** 037209
[9] Malashevich A and Vanderbilt D 2008 *Phys. Rev. Lett.* **101** 037210
[10] Shuvaev A M, Travkin V D, Ivanov V Y, Mukhin A A and Pimenov A 2010 *Phys. Rev. Lett.* **104** 097202
[11] Prokhnenko O, Aliouane N, Feyerherm R, Dudzik E, Wolter A U B, Maljuk A, Kiefer K and Argyriou D N 2010 *Phys. Rev.* B **81** 024419
[12] Rovillain P, Cazayous M, Gallais Y, Sacuto A, Measson M A and Sakata H 2010 *Phys. Rev.* B **81** 054428
[13] Jang H *et al* 2011 *Phys. Rev. Lett.* **106** 047203
[14] Kenzelmann M, Harris A B, Jonas S, Broholm C, Schefer J, Kim S B, Zhang C L, Cheong S W, Vajk O P and Lynn J W 2005 *Phys. Rev. Lett.* **95** 087206
[15] Katsura H, Nagaosa N and Balatsky A V 2005 *Phys. Rev. Lett.* **95** 057205
[16] Quezel S, Tcheou F, Rossat-Mignod J, Quezel G and Roudaut E 1977 *Physica* B + C **86–8** 916–8
[17] Kajimoto R, Yoshizawa H, Shintani H, Kimura T and Tokura Y 2004 *Phys. Rev.* B **70** 012401
[18] Wilkins S B *et al* 2009 *Phys. Rev. Lett.* **103** 207602
[19] Kimura T, Lawes G, Goto T, Tokura Y and Ramirez A P 2005 *Phys. Rev.* B **71** 224425
[20] Aliouane N, Schmalzl K, Senff D, Maljuk A, Prokeš K, Braden M and Argyriou D N 2009 *Phys. Rev. Lett.* **102** 207205
[21] Jin J L, Zhang X Q, Li G K, Cheng Z H, Zheng L and Lu Y 2011 *Phys. Rev.* B **83** 184431
[22] Cuartero V, Blasco J, Rodríguez -Velamazán J A, García J, Subías G, Ritter C, Stankiewicz J and Canadillas-Delgado L 2012 *Phys. Rev.* B **86** 104413
[23] Cui Y, Wang C and Cao B 2005 *Solid State Commun.* **133** 641–5
[24] Pavan Kumar N, Lalitha G and Venugopal Reddy P 2011 *Phys. Scr.* **83** 045701
[25] Ivanov V Yu, Mukhin A, Prokhorov A, Balbashov A and Iskhakova L 2010 *JETP Lett.* **91** 392–7
[26] Golosovsky I V, Mukhin A A, Ivanov V Yu, Vakhrushev S B, Golovenchits E I, Sanina V A, Hoffmann J -U, Feyerherm R and Dudzik E 2012 *Eur. Phys. J.* B **85** 1–6
[27] Blasco J, Ritter C, García J , de Teresa J M, Pérez-Cacho J and Ibarra M R 2000 *Phys. Rev.* B **62** 5609
[28] Senff D, Link P, Hradil K, Hiess A, Regnault L P, Sidis Y, Aliouane N, Argyriou D N and Braden M 2007 *Phys. Rev. Lett.* **98** 137206
[29] Kajimoto R, Mochizuki H, Yoshizawa H, Shintani H, Kimura T and Tokura Y 2005 *J. Phys. Soc. Japan* **74** 2430–3
[30] Bouvier M, Lethuillier P and Schmitt D 1991 *Phys. Rev.* B **43** 13137
[31] Mareschal J, Sivardière J, De Vries G F and Bertaut E F 1968 *J. Appl. Phys.* **39** 1364
[32] Tari A 2003 *The Specifc Heat of Matter at Low Temperatures* (London: Imperial College Press)
[33] Kopfermann H 1958 *Nuclear Moments* (New York: Academic)
[34] Woodfield B F, Wilson M L and Byers J M 1997 *Phys. Rev. Lett.* **78** 3201–4
[35] Lees M R, Petrenko O A, Balakrishnan G and Paul D M 1999 *Phys. Rev.* B **59** 1298–303
[36] Li Y, Graham R G, Ross J W, McCausland M A H, Bunbury D S P, Cao L, Kong L S and Shen B G 1996 *J. Phys. Condens. Matter* **8** 1059
[37] Vijayaraghavan R, Shimizu K, Itoh J, Grover A K and Gupta L C 1977 *J. Phys. Soc. Japan* **43** 1854–6
[38] Catanese C A, Skjeltorp A T, Meissner H E and Wolf W P 1973 *Phys. Rev.* B **8** 4223–46
[39] Germano D J and Butera R A 1981 *Phys. Rev.* B **24** 3912–27